



Article

# Synthesis, Structure, and Characterization of In<sub>10</sub>-Containing Open-Wells–Dawson Polyoxometalate

Satoshi Matsunaga, Takuya Otaki, Yusuke Inoue, Kohei Mihara and Kenji Nomiya \*

Department of Chemistry, Faculty of Science, Kanagawa University, Hiratsuka, Kanagawa 259-1293, Japan; matsunaga@kanagawa-u.ac.jp (S.M.); toatkaukyia1@gmail.com (T.O.); r201470042gl@jindai.jp (Y.I.); r201203938gu@jindai.jp (K.M.)

\* Correspondence: nomiya@kanagawa-u.ac.jp; Tel.: +81-463-59-4111

Academic Editor: Greta Ricarda Patzke

Received: 12 April 2016; Accepted: 10 May 2016; Published: 17 May 2016

**Abstract:** We have successfully synthesized  $K_{17}\{[\{KIn_2(\mu-OH)_2\}(\alpha,\alpha-Si_2W_{18}O_{66})]_2[In_6(\mu-OH)_{13}(H_2O)_8]\} \cdot 35H_2O$  (potassium salt of **In<sub>10</sub>-open**), an open-Wells–Dawson polyoxometalate (POM) containing ten indium metal atoms. This novel compound was characterized by X-ray crystallography, <sup>29</sup>Si NMR, FTIR, complete elemental analysis, and TG/DTA. X-ray crystallography results for  $\{[\{KIn_2(\mu-OH)_2\}(\alpha,\alpha-Si_2W_{18}O_{66})]_2[In_6(\mu-OH)_{13}(H_2O)_8]\}^{17-}$  (**In<sub>10</sub>-open**) revealed two open-Wells–Dawson units containing two In<sup>3+</sup> ions and a K<sup>+</sup> ion,  $[\{KIn_2(\mu-OH)_2\}(\alpha,\alpha-Si_2W_{18}O_{66})]^{11-}$ , connected by an In<sub>6</sub>-hydroxide cluster moiety,  $[In_6(\mu-OH)_{13}(H_2O)_8]^{5+}$ . **In<sub>10</sub>-open** is the first example of an open-Wells–Dawson POM containing a fifth-period element. Moreover, to the best of our knowledge, it exhibits the highest nuclearity among the indium-containing POMs reported to date.

**Keywords:** polyoxometalates; open-Wells–Dawson structural polyoxometalate; Indium

## 1. Introduction

Polyoxometalates (POMs) are discrete metal oxide clusters that are of current interest as soluble metal oxides, as well as for their application in catalysis, medicine, and materials science [1–13]. Recently, open-Wells–Dawson POMs have been reported as an emerging class of POMs [14–28]. These compounds are a dimerized species of the trilacunary Keggin POMs,  $[XW_9O_{34}]^{10-}$  (X = Si, Ge). Standard Wells–Dawson structural POMs are regarded as two trilacunary Keggin POM units assembled together via six W–O–W bonds. However, the electrostatic repulsion between the two units in  $[XW_9O_{34}]^{10-}$  (X = Si and Ge), induced by the highly charged guest  $XO_4^{4-}$  (X = Si, Ge) ion, is assumed to be so strong that it inhibits the assembly of the standard Wells–Dawson structure in aqueous media. Therefore, when the two trilacunary Keggin units comprise an  $XO_4^{4-}$  (X = Si, Ge) ion, they are linked by only two W–O–W bonds. This results in the formation of an open-Wells–Dawson structural POM [29]. The open pocket of these POMs can accommodate multiple metal ions (one to six metal ions). Thus, this class of compounds may constitute a promising platform for the development of metal-substituted-POM-based materials and catalysts. To date, many compounds that contain various metal ions in their open pocket, e.g., V<sup>5+</sup> [19], Mn<sup>2+</sup> [16,21], Fe<sup>3+</sup> [19], Co<sup>2+</sup> [14,16,20,21,25,27], Ni<sup>2+</sup> [16,21,24,27], Cu<sup>2+</sup> [15–17], and Zn<sup>2+</sup> [23] have been reported. Some lanthanoid (Eu<sup>3+</sup>, Gd<sup>3+</sup>, Tb<sup>3+</sup>, Dy<sup>3+</sup>, and Ho<sup>3+</sup>)-containing open-Wells–Dawson POMs have also been reported [22,26]. However, the large ionic radii of these lanthanoid atoms inhibit their complete insertion within the open pocket. This results in a weak coordination, similar to that of the K ions in K-containing open-Wells–Dawson POMs. Recently, we synthesized the Al<sub>4</sub>- and Ga<sub>4</sub>-containing open-Wells–Dawson POMs:  $[\{Al_4(\mu-OH)_6\}(\alpha,\alpha-Si_2W_{18}O_{66})]^{10-}$  (**Al<sub>4</sub>-open**) and  $[\{Ga_4(\mu-OH)_6\}(\alpha,\alpha-Si_2W_{18}O_{66})]^{10-}$  (**Ga<sub>4</sub>-open**), respectively, and successfully determined their molecular structures by single crystal X-ray crystallography [28]. X-ray structure analyses of **Al<sub>4</sub>-** and

**Ga<sub>4</sub>-open** revealed that the  $\{M_4(\mu\text{-OH})_6\}^{6+}$  ( $M = \text{Al}^{3+}, \text{Ga}^{3+}$ ) clusters are included in the open pocket of the open-Wells–Dawson unit.

In general, trivalent group 13 ions are found as various oligomeric hydroxide species in aqueous solution [30–32]. Synthetic and structural studies of group 13 ion-containing POMs provide informative and definitive molecular models of group 13 metal clusters in solution. However, among all the Al-, Ga-, and In-containing POMs, formed by the substitution of several tungsten ions in the parent POMs with trivalent group 13 ions [28,33–40], few well-characterized In-containing POMs have been reported to date [41–43]. Thus, In-containing POMs are intriguing target compounds from both a synthetic and a structural point of view.

In this study, we successfully synthesized an open-Wells–Dawson POM containing ten indium metal ions,  $\text{K}_{17}[\{\{\text{KIn}_2(\mu\text{-OH})_2\}(\alpha,\alpha\text{-Si}_2\text{W}_{18}\text{O}_{66})\}_2[\text{In}_6(\mu\text{-OH})_{13}(\text{H}_2\text{O})_8]\} \cdot 35\text{H}_2\text{O}$  (potassium salt of **In<sub>10</sub>-open**), and characterized it by X-ray crystallography, <sup>29</sup>Si NMR, FTIR, complete elemental analysis, and thermogravimetric/differential thermal analyses (TG/DTA). In contrast to **Al<sub>4</sub>-** and **Ga<sub>4</sub>-open**, **In<sub>10</sub>-open** showed a dimer structure bridged by a deca-indium-hydroxide cluster.

## 2. Results and Discussion

### 2.1. Synthesis

The crystalline sample of potassium salt of **In<sub>10</sub>-open**, was afforded in 17.9% yield. This complex was prepared from a 1:5 molar ratio reaction of  $\text{K}_{13}[\{\{\text{K}(\text{H}_2\text{O})_3\}_2\{\text{K}(\text{H}_2\text{O})_2\}(\alpha,\alpha\text{-Si}_2\text{W}_{18}\text{O}_{66})\}] \cdot 19\text{H}_2\text{O}$  with  $\text{InCl}_3$ . The sample was characterized using complete elemental analysis (H, In, K, O, Si, and W analyses), FTIR, TG/DTA, <sup>29</sup>Si NMR in D<sub>2</sub>O, and X-ray crystallography.

The FTIR spectrum of potassium salt of **In<sub>10</sub>-open** (Figure S1) displays peaks at 1000 and 945  $\text{cm}^{-1}$  that correspond to  $\nu_{\text{as}}(\text{Si-O})$  and  $\nu_{\text{as}}(\text{W-O}_t)$ , respectively. The characteristic bands at 900–600  $\text{cm}^{-1}$  are associated with  $\nu(\text{W-O}_c)$ ,  $\nu(\text{W-O}_b)$ , and  $\nu(\text{W-O-W})$ . The IR spectrum is very similar to those of the common open-Wells–Dawson POMs.

Before elemental analysis, the sample of **In<sub>10</sub>-open** was dried overnight at room temperature under vacuum ( $10^{-3}$ – $10^{-4}$  Torr). All elements (H, In, K, O, Si, and W) were observed for a total analysis of 100.37%. The recorded data were in good accordance with the calculated values for the formula without water of crystallization,  $\text{K}_{17}[\{\{\text{KIn}_2(\mu\text{-OH})_2\}(\alpha,\alpha\text{-Si}_2\text{W}_{18}\text{O}_{66})\}_2[\text{In}_6(\mu\text{-OH})_{13}(\text{H}_2\text{O})_8]$  (see Experimental section). The weight loss observed during drying, before analysis, was 5.28% corresponding to ca. 35 crystalline water molecules. On the other hand, during the TG/DTA measurements carried out under atmospheric conditions, a weight loss of 6.40%, observed at temperatures below 500 °C, corresponding to a total of ca. 42 water molecules, *i.e.*, 8 coordinated water molecules and 34 molecules of water of crystallization (Figure S2). Thus, the elemental analysis and TG/DTA displayed a presence of a total of 34–35 water molecules for the sample under atmospheric conditions. The formula for potassium salt of **In<sub>10</sub>-open** presented herein was determined as  $\text{K}_{17}[\{\{\text{KIn}_2(\mu\text{-OH})_2\}(\alpha,\alpha\text{-Si}_2\text{W}_{18}\text{O}_{66})\}_2[\text{In}_6(\mu\text{-OH})_{13}(\text{H}_2\text{O})_8] \cdot 35\text{H}_2\text{O}$  based on the results of the complete elemental analysis.

### 2.2. Molecular Structure

The molecular structure of the polyoxoanion of potassium salt of **In<sub>10</sub>-open** and its polyhedral representation are shown in Figure 1a,b, respectively. X-ray crystallographic data of **In<sub>10</sub>-open** reveal that the two open-Wells–Dawson units that include two  $\text{In}^{3+}$  ions and a  $\text{K}^+$  ion,  $[\{\{\text{KIn}_2(\mu\text{-OH})_2\}(\alpha,\alpha\text{-Si}_2\text{W}_{18}\text{O}_{66})\}]^{11-}$ , are connected by a central  $\text{In}_6$ -hydroxide cluster moiety,  $[\text{In}_6(\mu\text{-OH})_{13}(\text{H}_2\text{O})_8]^{5+}$ , to form a dimeric open-Wells–Dawson polyanion,  $\{[\{\{\text{KIn}_2(\mu\text{-OH})_2\}(\alpha,\alpha\text{-Si}_2\text{W}_{18}\text{O}_{66})\}_2[\text{In}_6(\mu\text{-OH})_{13}(\text{H}_2\text{O})_8]\}^{17-}$  (Figure 1).

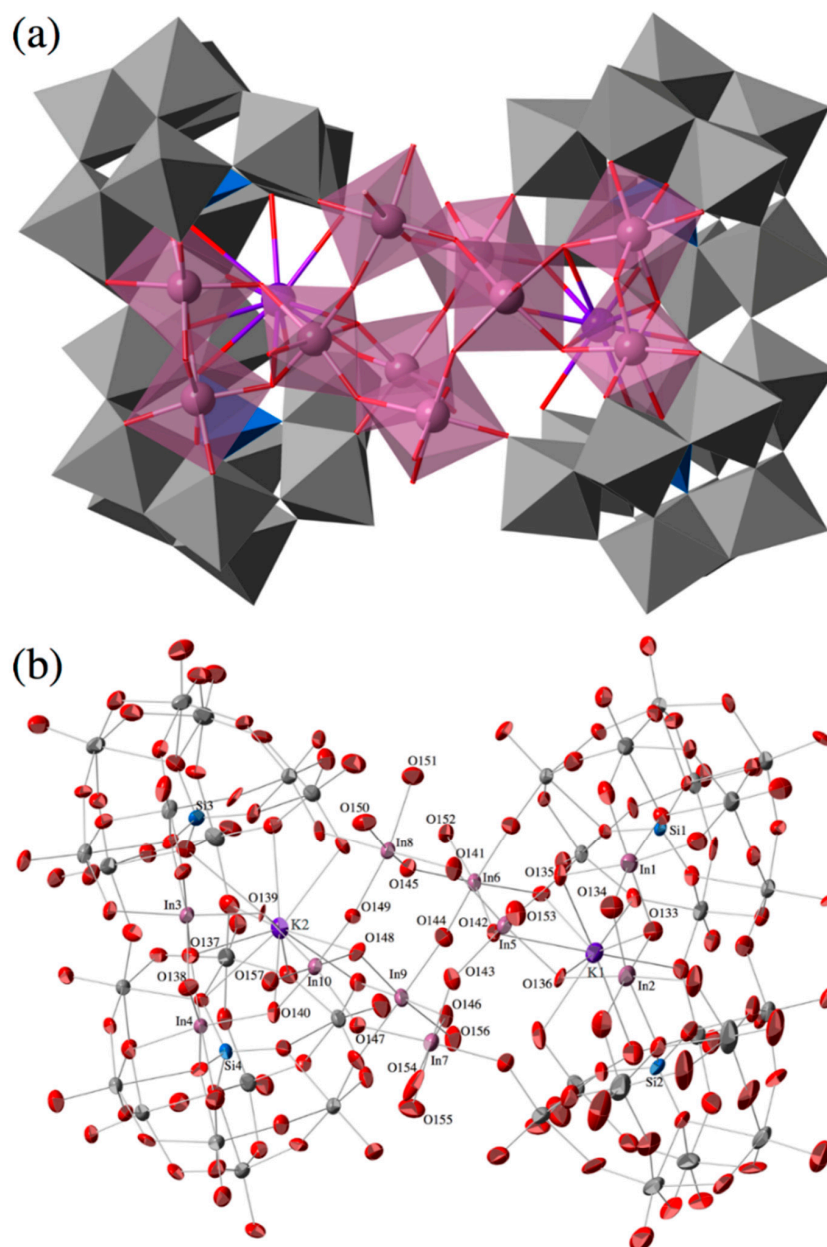


**Figure 1.** Molecular structure of the polyoxoanion,  $\{[\{KIn_2(\mu-OH)_2\}(\alpha,\alpha-Si_2W_{18}O_{66})]_2[In_6(\mu-OH)_{13}(H_2O)_8]\}^{17-}$  of potassium salt of **In<sub>10</sub>-open**. (a) Its polyhedral representation; and (b) thermal ellipsoidal plot. Color code: In, pink; K, purple; O, red; Si, blue; W, gray.

The two indium atoms in the open pocket of the open-Wells–Dawson POM units are connected through edge-sharing oxygen atoms (O133, O134 for In1, In2; O137, O138 for In3, In4) with In···In distances of 3.266(2) (In1···In2) and 3.299(2) (In3···In4) (Figure 2a). Each Indium atom in the open pocket is bonded to three oxygen atoms of the lacunary site in the open-Wells–Dawson polyanion [In–O average = 2.2011 Å]. Open-Wells–Dawson POMs that include two metal atoms in the open pocket have been previously reported, e.g.,  $K_{11}[\{KV_2O_3(H_2O)_2\}(Si_2W_{18}O_{66})] \cdot 40H_2O$  (**V<sub>2</sub>-open**) [19]. In contrast to our **In<sub>10</sub>-open**, the two vanadium atoms in the open pocket of **V<sub>2</sub>-open** are bound to only one half {SiW<sub>9</sub>} of the open-Wells–Dawson unit, and are linked in a corner-sharing fashion (Figure 2b). Therefore, **In<sub>10</sub>-open** is the first example of an open-Wells–Dawson POM that includes two metal atoms with edge-sharing fashion.

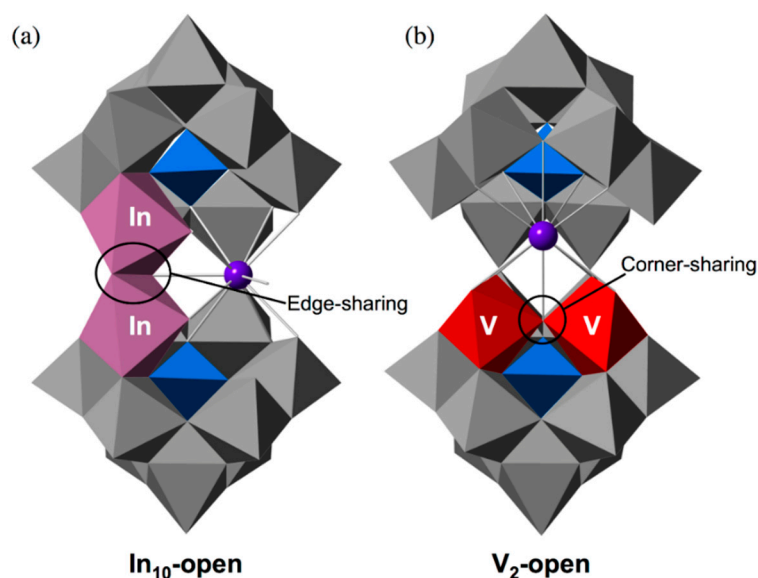


**Figure 2.** The metal arrangement of (a) **In<sub>10</sub>-open** and (b) **V<sub>2</sub>-open** in the open pocket.

In addition to the indium atoms in the open-pocket, the complex contains six indium atoms in the bridging hydroxide cluster. The indium atoms in the bridging cluster are connected to each other in a corner-sharing fashion. Moreover, the In atoms in the open-pocket and the W atoms of the open-Wells–Dawson POM units are also linked to the In atoms of the bridging cluster in a corner-sharing fashion. Thus, all the Indium atoms can be considered to be 6-coordinated. Bond valence sum (BVS) [44] calculations suggest that the corner- and edge-sharing oxygen atoms that are linked to the In atoms (corner-sharing: O135, O136, O139, O140, O141, O142, O143, O144, O145, O146, O147, O148, and O149; edge-sharing: O133, O134, O137, and O138) are protonated, *i.e.*, they are ascribed to the hydroxide groups. On the other hand, the terminal oxygen atoms on the indium atoms (O150, O151, O152, O153, O154, O155, O156, and O157) are ascribed to the water groups (Table S1).

**In<sub>10</sub>-open** has a dimeric structure composed of two indium-containing open-Wells–Dawson POM moieties bridged by In<sub>6</sub> hydroxide clusters. Dimeric open-Wells–Dawson POMs, similar to **In<sub>10</sub>-open**, have also been reported for  $\{[\text{Zn}_6(\mu\text{-OH})_7(\text{H}_2\text{O})(\alpha,\alpha\text{-Si}_2\text{W}_{18}\text{O}_{66})]_2\}^{22-}$  (**Zn<sub>12</sub>-open**) by Hill *et al.* [23]. In this complex, the six zinc atoms are included in the open pocket of the open-Wells–Dawson unit, and the two Zn<sub>6</sub>-containing open-Wells–Dawson units are connected through the two edge-sharing oxygen atoms. The arrangement and the number of metal ions in the open-pocket of the **In<sub>10</sub>-open** are different from those of the **Zn<sub>12</sub>-open** reported previously.

In open-Wells–Dawson POMs, the bite angle can be defined as the dihedral angle between the planes that pass through the six oxygen atoms of the lacunary site of each trilacunary Keggin unit. The bite angle varies, depending on the metal cluster included in the open pocket of the open-Wells–Dawson unit. The bite angles of **In<sub>10</sub>-open** are 64.363° and 65.139° (Figure 3). These values are wider than those of other open-Wells–Dawson POMs, including other group 13 ions, such as **Al<sub>4</sub>-** (54.274°) and **Ga<sub>4</sub>-open** (56.110°) [28]. The difference between the bite angles of **Al<sub>4</sub>-**, **Ga<sub>4</sub>-**, and **In<sub>10</sub>-open** is caused by the difference in the ionic radii of the Al (0.53 Å), Ga (0.76 Å), and In (0.94 Å) ions [45,46]. **In<sub>10</sub>-open** displays the widest bite angles when compared to previously reported open-Wells–Dawson POMs, including the Co<sub>6</sub> (60.045°) [27], Zn<sub>6</sub> dimer (60.308°) [23], Ni<sub>5</sub> (58.925°) [24], and Cu<sub>5</sub> (61.663°) [15,17] clusters. The open-Wells–Dawson POM containing a Cu<sub>5</sub> cluster (**Cu<sub>5</sub>-open**) exhibits a large bite angle (61.663°) due to the long bond lengths between the copper and the edge-sharing oxygen atom, caused by Jahn–Teller distortion [15,17]. The bite angles of **In<sub>10</sub>-open** are ca. 3° wider than that of **Cu<sub>5</sub>-open**. This increase appears to be caused by the large ionic radius of the indium ions incorporated in the open pocket.

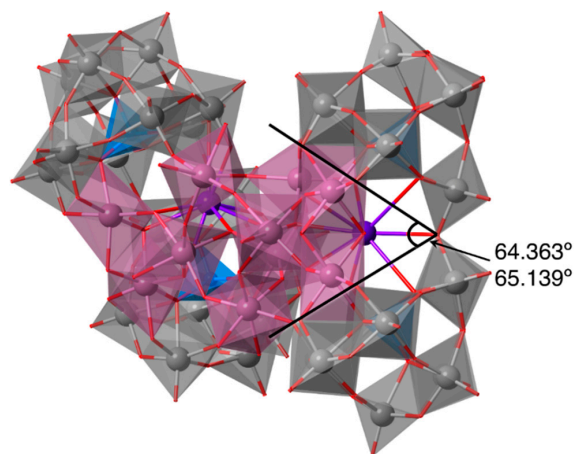


Figure 3. Bite angles of **In<sub>10</sub>-open**.

The previously reported open-Wells–Dawson POMs mainly accommodated the fourth-period elements. Except for the lanthanoid-containing open-Wells–Dawson POMs, whose open-pockets weakly coordinate to the lanthanoid ions, open-Wells–Dawson POMs that accommodate the larger fifth- and sixth-period elements have not been reported to date. Thus, **In<sub>10</sub>-open** indicates that elements (such as indium) having large ionic radii (0.94 Å) can be incorporated in the open-pocket of an open-Wells–Dawson unit.

### 2.3. Solution <sup>29</sup>Si NMR

The solution <sup>29</sup>Si NMR spectrum of **In<sub>10</sub>-open** in D<sub>2</sub>O displays a two-line spectrum at −82.415 and −83.159 ppm in a 1:1 ratio (Figure 4). The two Si atoms in one open-Wells–Dawson unit are nonequivalent due to the configuration of the other open-Wells–Dawson unit, even though the two units are equivalent. The adjacent two <sup>29</sup>Si NMR peaks are consistent with the structure of **In<sub>10</sub>-open** observed by X-ray crystallography. This suggests that **In<sub>10</sub>-open** exists as a single species and maintains its structure in solution.

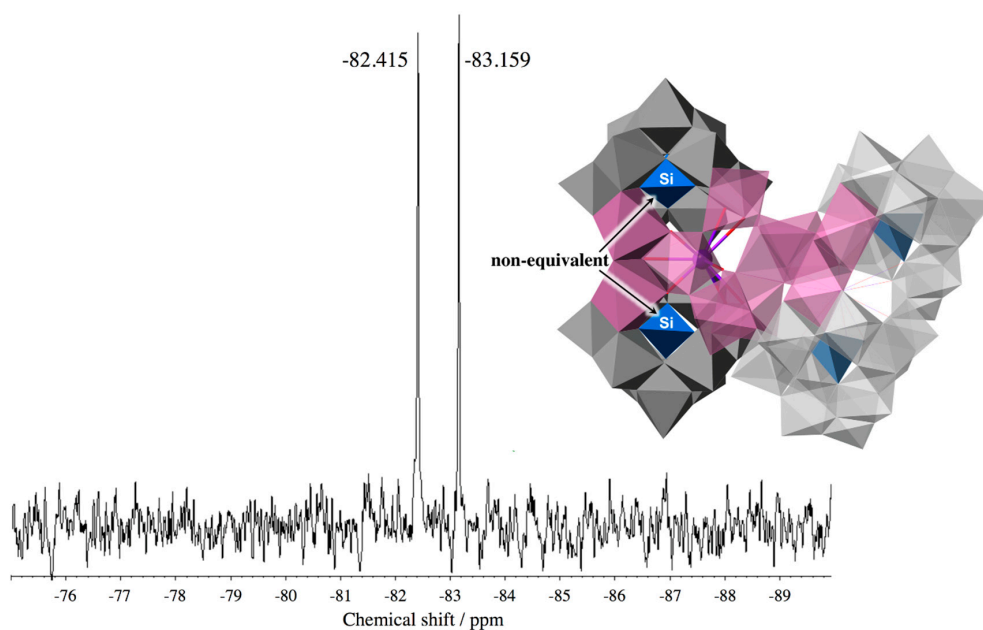


Figure 4. Solution <sup>29</sup>Si NMR spectrum of potassium salt of **In<sub>10</sub>-open** dissolved in D<sub>2</sub>O.

### 3. Experimental Section

#### 3.1. Materials

The following reagents were used as received:  $\text{InCl}_3$  (from Sigma-Aldrich Japan, Shinagawa, Japan),  $\text{KOH}$ ,  $\text{KCl}$  (from Wako Pure Chemical Industries, Osaka, Japan), and  $\text{D}_2\text{O}$  (Kanto Chemical, Tokyo, Japan). The K ion-incorporating open-Wells–Dawson POM,  $\text{K}_{13}[\{\text{K}(\text{H}_2\text{O})_3\}_2\{\text{K}(\text{H}_2\text{O})_2\}(\alpha,\alpha\text{-Si}_2\text{W}_{18}\text{O}_{66})\}\cdot 19\text{H}_2\text{O}$ , was prepared according to literature [14], and identified by TG/DTA and FT-IR analysis.

#### 3.2. Instrumentation and Analytical Procedures

A complete elemental analysis was carried out by Mikroanalytisches Labor Pascher (Remagen, Germany). The sample was dried overnight at room temperature under a pressure of  $10^{-3}$ – $10^{-4}$  Torr before analysis. The  $^{29}\text{Si}$  NMR (119.24 MHz) spectra in  $\text{D}_2\text{O}$  solution were recorded in 5-mm outer diameter tubes, on a JEOL JNM ECP 500 FTNMR spectrometer with a JEOL ECP-500 NMR data-processing system (JEOL, Akishima, Japan). The  $^{29}\text{Si}$  NMR spectrum was referenced to an internal standard of DSS. Infrared spectra were recorded on a Jasco 4100 FTIR spectrometer (Jasco, Hachioji, Japan) by using KBr disks at room temperature. TG/DTA measurements were performed using a Rigaku Thermo Plus 2 series TG8120 instrument (Rigaku, Akishima, Japan), under air flow with a temperature ramp of 4.0 °C per min at a temperature ranging between 26 and 500 °C.

#### 3.3. Synthesis of $\text{K}_{17}[\{\{\text{KIn}_2(\mu\text{-OH})_2\}(\alpha,\alpha\text{-Si}_2\text{W}_{18}\text{O}_{66})\}_2[\text{In}_6(\mu\text{-OH})_{13}(\text{H}_2\text{O})_8]\}\cdot 35\text{H}_2\text{O}$ (Potassium Salt of **In<sub>10</sub>-open**)

$\text{InCl}_3$  (398 mg, 1.80 mmol) was dissolved in water (40 mL). A separate solution of  $\text{K}_{13}[\{\text{K}(\text{H}_2\text{O})_3\}_2\{\text{K}(\text{H}_2\text{O})_2\}(\alpha,\alpha\text{-Si}_2\text{W}_{18}\text{O}_{66})\}\cdot 19\text{H}_2\text{O}$  (2.00 g, 0.361 mmol) dissolved in 100 mL of distilled water was added dropwise to the resulting solution. The pH of this solution was adjusted to 4.0 using 0.1 M  $\text{KOH}_{\text{aq}}$ . Next, 4 mL of saturated  $\text{KCl}_{\text{aq}}$  were added to the solution. The resulting solution was left to stand undisturbed at room temperature for 3 days. The afforded colorless needle crystals were collected on a membrane filter (JG 0.2  $\mu\text{m}$ ), and dried *in vacuo* for 2 h. Yield = 0.381 g (0.0323 mmol, 17.9% based on  $\text{K}_{13}[\{\text{K}(\text{H}_2\text{O})_3\}_2\{\text{K}(\text{H}_2\text{O})_2\}(\alpha,\alpha\text{-Si}_2\text{W}_{18}\text{O}_{66})\}\cdot 19\text{H}_2\text{O}$ ).

The crystalline sample was soluble in water, but insoluble in organic solvents such as methanol, ethanol, and diethyl ether. Elemental analysis (%) calcd. for  $\text{H}_{33}\text{In}_{10}\text{K}_{19}\text{O}_{157}\text{Si}_4\text{W}_{36}$  or  $\text{K}_{17}[\{\{\text{KIn}_2(\mu\text{-OH})_2\}(\alpha,\alpha\text{-Si}_2\text{W}_{18}\text{O}_{66})\}_2[\text{In}_6(\mu\text{-OH})_{13}(\text{H}_2\text{O})_8]\}\cdot 34\text{H}_2\text{O}$ ; IR (KBr,  $\text{cm}^{-1}$ ): 1622 (m), 1000 (w), 945 (m), 890 (vs), 786 (vs), 730 (vs), 649 (s), 548 (m), 523 (m);  $^{29}\text{Si}$  NMR (50.0 °C,  $\text{D}_2\text{O}$ , DSS, ppm):  $\delta = -82.415, -83.159$ .

#### 3.4. X-Ray Crystallography

For **In<sub>10</sub>-open**, a single crystal with dimensions of  $0.21 \times 0.06 \times 0.05 \text{ mm}^3$  was surrounded by liquid paraffin (Paratone-N) and analyzed at 150(2) K. All measurements were performed on a Rigaku MicroMax-007HF with a Saturn CCD diffractometer (Rigaku). The structure was solved by direct methods (SHELXS-97), followed by difference Fourier calculations and refinement by a full-matrix least-squares procedure on  $F^2$  (program SHELXL-97) [47].

Crystal data: monoclinic, space group  $\text{P}2(1)/a$ ,  $a = 23.525(5)$ ,  $b = 32.926(7)$ ,  $c = 25.424(6)$  Å,  $\beta = 93.273(2)^\circ$ ,  $V = 19661(7)$  Å<sup>3</sup>,  $Z = 4$ ,  $D_{\text{calcd}} = 3.857 \text{ g cm}^{-3}$ ,  $\mu(\text{Mo-K}\alpha) = 22.491 \text{ mm}^{-1}$ ;  $R_1[I > 2.00\sigma(I)] = 0.0829$ ,  $R$  (all data) = 0.1012,  $wR_2$  (all data) = 0.2296, GOF = 1.056. Most atoms

in the main part of the structure were refined anisotropically, while the rest (as crystallization solvents) were refined isotropically, because of the presence of disorder. The composition and formula of the POM (containing many countercations and many crystalline water molecules) were determined from complete elemental and TG analyses. Similar to structural investigations of other crystals of highly hydrated large POM complexes, it was not possible to locate every countercation and hydrated water molecule in the complex. This frequently encountered situation is attributed to the extensive disorder of the cations and many of the crystalline water molecules. Further details on the crystal structure investigations may be obtained from: Fachinformationszentrum Karlsruhe, 76344 Eggenstein-Leopoldshafen, Germany (Fax: +49-7247-808-666; E-Mail: crysdata@fiz-karlsruhe.de, [http://www.fiz-karlsruhe.de/request\\_for\\_deposited\\_data.html?&L=1](http://www.fiz-karlsruhe.de/request_for_deposited_data.html?&L=1)) on quoting the depository number CSD-430962 (Identification code; 56\_11\_1).

#### 4. Conclusions

In summary, we prepared and characterized an open-Wells–Dawson structural POM, potassium salt of **In<sub>10</sub>-open**, containing ten indium ions, *i.e.*,  $K_{17}\{[\{KIn_2(\mu-OH)_2\}(\alpha,\alpha-Si_2W_{18}O_{66})]_2 [In_6(\mu-OH)_{13}(H_2O)_8]\} \cdot 35H_2O$  (potassium salt of **In<sub>10</sub>-open**). Single-crystal X-ray analyses revealed that two open-Wells–Dawson units that include two  $In^{3+}$  ions and a  $K^+$  ion are connected by an  $In_6$ -hydroxide cluster moiety to form a dimeric open-Wells–Dawson polyanion. **In<sub>10</sub>-open** displayed the widest bite angles among the previously reported open-Wells–Dawson POMs. This is mainly due to the large ionic radius of the indium ion. The solution  $^{29}Si$  spectrum in  $D_2O$  indicated that **In<sub>10</sub>-open** was obtained as a single species and that its structure was maintained in solution. **In<sub>10</sub>-open** is the first example of an open-Wells–Dawson POM containing a fifth-period element, and it exhibits the highest nuclearity of any indium-containing POM reported to date. This work can be extended to the future molecular design of novel open-Wells–Dawson POMs containing large fifth- and sixth-period elements, such as Ru, Rh, Pd, Pt. Studies of open-Wells–Dawson structural POMs containing larger metal atoms are in progress.

**Supplementary Materials:** The following are available online at [www.mdpi.com/2304-6740/4/2/16/s1](http://www.mdpi.com/2304-6740/4/2/16/s1), Figure S1: FT-IR spectrum of potassium salt of **In<sub>10</sub>-open** (KBr disk), Figure S2: TG/DTA data of potassium salt of **In<sub>10</sub>-open** (from 22 to 500 °C), Table S1: Bond valence sum (BVS) calculations of In and O atoms of the Indium-cluster moieties of **In<sub>10</sub>-open**: checkCIF/PLATON report.

**Acknowledgments:** This study was supported by the Strategic Research Base Development Program for Private Universities of the Ministry of Education, Culture, Sports, Science and Technology of Japan, and also by a grant from the Research Institute for Integrated Science, Kanagawa University (RIIS201505).

**Author Contributions:** Satoshi Matsunaga and Kenji Nomiya conceived and designed the experiments, and wrote the paper; Takuya Otaki and Yusuke Inoue synthesized and characterized the compound; Kohei Mihara assisted characterization of the compound.

**Conflicts of Interest:** The authors declare no conflict of interest.

#### Abbreviations

The following abbreviations are used in this manuscript:

POM	Polyoxometalate
TG/DTA	Thermogravimetric/differential thermal analyses
BVS	Bond valence sum

#### References

1. Pope, M.T.; Müller, A. Polyoxometalate chemistry: An old field with new dimensions in several disciplines. *Angew. Chem. Int. Ed.* **1991**, *30*, 34–48. [[CrossRef](#)]
2. Pope, M.T. *Heteropoly- and Isopolyoxometalates*; Springer-Verlag: New York, NY, USA, 1983.
3. Hill, C.L.; Prosser-McCartha, C.M. Homogeneous catalysis by transition metal oxygen anion clusters. *Coord. Chem. Rev.* **1995**, *143*, 407–455. [[CrossRef](#)]

4. Neumann, R. Polyoxometalate complexes in organic oxidation chemistry. *Prog. Inorg. Chem.* **1998**, *47*, 317–370.
5. Proust, A.; Thouvenot, R.; Gouzerh, P. Functionalization of polyoxometalates: Towards advanced applications in catalysis and materials science. *Chem. Commun.* **2008**, 1837–1852. [[CrossRef](#)] [[PubMed](#)]
6. Hasenknopf, B.; Micoine, K.; Lacôte, E.; Thorimbert, S.; Malacria, M.; Thouvenot, R. Chirality in polyoxometalate chemistry. *Eur. J. Inorg. Chem.* **2008**, *2008*, 5001–5013. [[CrossRef](#)]
7. Long, D.-L.; Tsunashima, R.; Cronin, L. Polyoxometalates: Building blocks for functional nanoscale systems. *Angew. Chem. Int. Ed.* **2010**, *49*, 1736–1758. [[CrossRef](#)] [[PubMed](#)]
8. Nomiya, K.; Sakai, Y.; Matsunaga, S. Chemistry of group IV metal ion-containing polyoxometalates. *Eur. J. Inorg. Chem.* **2011**, *2011*, 179–196. [[CrossRef](#)]
9. Izarova, N.V.; Pope, M.T.; Kortz, U. Noble metals in polyoxometalates. *Angew. Chem. Int. Ed.* **2012**, *51*, 9492–9510. [[CrossRef](#)] [[PubMed](#)]
10. Song, Y.-F.; Tsunashima, R. Recent advances on polyoxometalate-based molecular and composite materials. *Chem. Soc. Rev.* **2012**, *41*, 7384–7402. [[CrossRef](#)] [[PubMed](#)]
11. Bijelic, A.; Rompel, A. The use of polyoxometalates in protein crystallography—An attempt to widen a well-known bottleneck. *Coord. Chem. Rev.* **2015**, *299*, 22–38. [[CrossRef](#)] [[PubMed](#)]
12. Wang, S.-S.; Yang, G.-Y. Recent advances in polyoxometalate-catalyzed reactions. *Chem. Rev.* **2015**, *115*, 4893–4962. [[CrossRef](#)] [[PubMed](#)]
13. Blazevic, A.; Rompel, A. The Anderson–Evans polyoxometalate: From inorganic building blocks via hybrid organic–inorganic structures to tomorrows “Bio-POM”. *Coord. Chem. Rev.* **2016**, *307*, 42–64. [[CrossRef](#)]
14. Laronze, N.; Marrot, J.; Hervé, G. Synthesis, molecular structure and chemical properties of a new tungstosilicate with an open Wells–Dawson structure,  $\alpha$ -[Si<sub>2</sub>W<sub>18</sub>O<sub>66</sub>]<sup>16-</sup>. *Chem. Commun.* **2003**, *21*, 2360–2361. [[CrossRef](#)]
15. Bi, L.-H.; Kortz, U. Synthesis and structure of the pentacopper(II) substituted tungstosilicate [Cu<sub>5</sub>(OH)<sub>4</sub>(H<sub>2</sub>O)<sub>2</sub>(A- $\alpha$ -SiW<sub>9</sub>O<sub>33</sub>)<sub>2</sub>]<sup>10-</sup>. *Inorg. Chem.* **2004**, *43*, 7961–7962. [[CrossRef](#)] [[PubMed](#)]
16. Leclerc-Laronze, N.; Marrot, J.; Hervé, G. Cation-directed synthesis of tungstosilicates. 2. Synthesis, structure, and characterization of the open Wells–Dawson anion  $\alpha$ -[K(H<sub>2</sub>O)<sub>2</sub>(Si<sub>2</sub>W<sub>18</sub>O<sub>66</sub>)]<sup>15-</sup> and its transition-metal derivatives [M(H<sub>2</sub>O)](μ-H<sub>2</sub>O)<sub>2</sub>K(Si<sub>2</sub>W<sub>18</sub>O<sub>66</sub>)]<sup>13-</sup> and [M(H<sub>2</sub>O)](μ-H<sub>2</sub>O)<sub>2</sub>K{M(H<sub>2</sub>O)<sub>4</sub>(Si<sub>2</sub>W<sub>18</sub>O<sub>66</sub>)]<sup>11-</sup>. *Inorg. Chem.* **2005**, *44*, 1275–1281. [[PubMed](#)]
17. Nellutla, S.; Tol, J.V.; Dalal, N.S.; Bi, L.-H.; Kortz, U.; Keita, B.; Nadjo, L.; Khitrov, G.A.; Marshall, A.G. Magnetism, electron paramagnetic resonance, electrochemistry, and mass spectrometry of the pentacopper(II)-substituted tungstosilicate [Cu<sub>5</sub>(OH)<sub>4</sub>(H<sub>2</sub>O)<sub>2</sub>(A- $\alpha$ -SiW<sub>9</sub>O<sub>33</sub>)<sub>2</sub>]<sup>10-</sup>, A model five-spin frustrated cluster. *Inorg. Chem.* **2005**, *44*, 9795–9806. [[CrossRef](#)] [[PubMed](#)]
18. Leclerc-Laronze, N.; Haouas, M.; Marrot, J.; Taulelle, F.; Hervé, G. Step-by-step assembly of trivacant tungstosilicates: Synthesis and characterization of tetrameric anions. *Angew. Chem. Int. Ed.* **2006**, *45*, 139–142. [[CrossRef](#)] [[PubMed](#)]
19. Leclerc-Laronze, N.; Marrot, J.; Hervé, G. Dinuclear vanadium and tetranuclear iron complexes obtained with the open Wells–Dawson [Si<sub>2</sub>W<sub>18</sub>O<sub>66</sub>]<sup>16-</sup> tungstosilicate. *C. R. Chim.* **2006**, *9*, 1467–1471. [[CrossRef](#)]
20. Sun, C.-Y.; Liu, S.-X.; Wang, C.-L.; Xie, L.-H.; Zhang, C.-D.; Gao, B.; Su, Z.-M.; Jia, H.-Q. Synthesis, structure and characterization of a new cobalt-containing germanotungstate with open Wells–Dawson structure: K<sub>13</sub>[{Co(H<sub>2</sub>O)}(μ-H<sub>2</sub>O)<sub>2</sub>K(Ge<sub>2</sub>W<sub>18</sub>O<sub>66</sub>)]. *J. Mol. Struct.* **2006**, *785*, 170–175. [[CrossRef](#)]
21. Wang, C.-L.; Liu, S.-X.; Sun, C.-Y.; Xie, L.-H.; Ren, Y.-H.; Liang, D.-D.; Cheng, H.-Y. Bimetals substituted germanotungstate complexes with open Wells–Dawson structure: Synthesis, structure, and electrochemical behavior of [M(H<sub>2</sub>O)](μ-H<sub>2</sub>O)<sub>2</sub>K{M(H<sub>2</sub>O)<sub>4</sub>(Ge<sub>2</sub>W<sub>18</sub>O<sub>66</sub>)]<sup>11-</sup> (M = Co, Ni, Mn). *J. Mol. Struct.* **2007**, *841*, 88–95. [[CrossRef](#)]
22. Ni, L.; Hussain, F.; Spingler, B.; Weyeneth, S.; Patzke, G.R. Lanthanoid-containing open Wells–Dawson silicotungstates: Synthesis, crystal structures, and properties. *Inorg. Chem.* **2011**, *50*, 4944–4955. [[CrossRef](#)] [[PubMed](#)]
23. Zhu, G.; Geletii, Y.V.; Zhao, C.; Musaev, D.G.; Song, J.; Hill, C.L. A dodecanuclear Zn cluster sandwiched by polyoxometalate ligands. *Dalton Trans.* **2012**, *41*, 9908–9913. [[CrossRef](#)] [[PubMed](#)]
24. Zhu, G.; Glass, E.N.; Zhao, C.; Lv, H.; Vickers, J.W.; Geletii, Y.V.; Musaev, D.G.; Song, J.; Hill, C.L. A nickel containing polyoxometalate water oxidation catalyst. *Dalton Trans.* **2012**, *41*, 13043–13049. [[CrossRef](#)] [[PubMed](#)]

25. Zhu, G.; Geletii, Y.V.; Song, J.; Zhao, C.; Glass, E.N.; Bacsá, J.; Hill, C.L. Di- and tri-cobalt silicotungstates: Synthesis, characterization, and stability studies. *Inorg. Chem.* **2013**, *52*, 1018–1024. [[CrossRef](#)] [[PubMed](#)]
26. Ni, L.; Spingler, B.; Weyeneth, S.; Patzke, G.R. Trilacunary Keggin-type POMs as versatile building blocks for lanthanoid silicotungstates. *Eur. J. Inorg. Chem.* **2013**, *2013*, 1681–1692. [[CrossRef](#)]
27. Guo, J.; Zhang, D.; Chen, L.; Song, Y.; Zhu, D.; Xu, Y. Syntheses, structures and magnetic properties of two unprecedented hybrid compounds constructed from open Wells–Dawson anions and high-nuclear transition metal clusters. *Dalton Trans.* **2013**, *42*, 8454–8459. [[CrossRef](#)] [[PubMed](#)]
28. Matsunaga, S.; Inoue, Y.; Otaki, T.; Osada, H.; Nomiya, K. Aluminum- and gallium-containing open-Dawson polyoxometalates. *Z. Anorg. Allg. Chem.* **2016**, *642*, 539–545. [[CrossRef](#)]
29. Zhang, F.-Q.; Guan, W.; Yan, L.-K.; Zhang, Y.-T.; Xu, M.-T.; Hayfron-Benjamin, E.; Su, Z.-M. On the origin of the relative stability of Wells–Dawson isomers: A DFT study of  $\alpha$ -,  $\beta$ -,  $\gamma$ -,  $\alpha^*$ -,  $\beta^*$ -, and  $\gamma^*$ -[(PO<sub>4</sub>)<sub>2</sub>W<sub>18</sub>O<sub>54</sub>]<sup>6-</sup> anions. *Inorg. Chem.* **2011**, *50*, 4967–4977. [[CrossRef](#)] [[PubMed](#)]
30. Jordan, P.A.; Clayden, N.J.; Heath, S.L.; Moore, G.R.; Powell, A.K.; Tapparo, A. Defining speciation profiles of Al<sup>3+</sup> complexed with small organic ligands: The Al<sup>3+</sup>-heidi system. *Coord. Chem. Rev.* **1996**, *149*, 281–309. [[CrossRef](#)]
31. Casey, W.H. Large aqueous aluminum hydroxide molecules. *Chem. Rev.* **2006**, *106*, 1–16. [[CrossRef](#)] [[PubMed](#)]
32. Mensinger, Z.L.; Wang, W.; Keszler, D.A.; Johnson, D.W. Oligomeric group 13 hydroxide compounds—A rare but varied class of molecules. *Chem. Soc. Rev.* **2012**, *41*, 1019–1030. [[CrossRef](#)] [[PubMed](#)]
33. Kikukawa, Y.; Yamaguchi, S.; Nakagawa, Y.; Uehara, K.; Uchida, S.; Yamaguchi, K.; Mizuno, N. Synthesis of a dialuminum-substituted silicotungstate and the diastereoselective cyclization of citronellal derivatives. *J. Am. Chem. Soc.* **2008**, *130*, 15872–15878. [[CrossRef](#)] [[PubMed](#)]
34. Kato, C.N.; Katayama, Y.; Nagami, M.; Kato, M.; Yamasaki, M. A sandwich-type aluminium complex composed of tri-lacunary Keggin-type polyoxotungstate: Synthesis and X-ray crystal structure of [(A-PW<sub>9</sub>O<sub>34</sub>)<sub>2</sub>{W(OH)(OH<sub>2</sub>)}{Al(OH)(OH<sub>2</sub>)}{Al( $\mu$ -OH)(OH<sub>2</sub>)<sub>2</sub>}]<sup>7-</sup>. *Dalton Trans.* **2010**, *39*, 11469–11474. [[CrossRef](#)] [[PubMed](#)]
35. Kikukawa, Y.; Yamaguchi, K.; Hibino, M.; Mizuno, N. Layered assemblies of a dialuminum-substituted silicotungstate trimer and the reversible interlayer cation-exchange properties. *Inorg. Chem.* **2011**, *50*, 12411–12413. [[CrossRef](#)] [[PubMed](#)]
36. Carraro, M.; Bassil, B.S.; Sorarù, A.; Berardi, S.; Suchopar, A.; Kortz, U.; Bonchio, M. A Lewis acid catalytic core sandwiched by inorganic polyoxoanion caps: Selective H<sub>2</sub>O<sub>2</sub>-based oxidations with [Al<sup>III</sup><sub>4</sub>(H<sub>2</sub>O)<sub>10</sub>( $\beta$ -XW<sub>9</sub>O<sub>33</sub>H)<sub>2</sub>]<sup>6-</sup> (X = As<sup>III</sup>, Sb<sup>III</sup>). *Chem. Commun.* **2013**, *49*, 7914–7916. [[CrossRef](#)] [[PubMed](#)]
37. Kato, C.N.; Makino, Y.; Unno, W.; Uno, H. Synthesis, molecular structure, and stability of a zirconocene derivative with  $\alpha$ -Keggin mono-aluminum substituted polyoxotungstate. *Dalton Trans.* **2013**, *42*, 1129–1135. [[CrossRef](#)] [[PubMed](#)]
38. Kato, C.N.; Kashiwagi, T.; Unno, W.; Nakagawa, M.; Uno, H. Syntheses and molecular structures of monomeric and hydrogen-bonded dimeric Dawson-type trialuminum-substituted polyoxotungstates derived under acidic and basic conditions. *Inorg. Chem.* **2014**, *53*, 4823–4832. [[CrossRef](#)] [[PubMed](#)]
39. Inoue, Y.; Matsunaga, S.; Nomiya, K. Al<sub>16</sub>-hydroxide cluster-containing tetrameric polyoxometalate, [( $\alpha$ -Al<sub>3</sub>SiW<sub>9</sub>O<sub>34</sub>( $\mu$ -OH)<sub>6</sub>]<sub>4</sub>{Al<sub>4</sub>( $\mu$ -OH)<sub>6</sub>}]<sup>22-</sup>. *Chem. Lett.* **2015**, *44*, 1649–1651. [[CrossRef](#)]
40. Allmen, K.; Car, P.-E.; Blacque, O.; Fox, T.; Müller, R.; Patzke, G.R. Structure and properties of new gallium-containing polyoxotungstates with hexanuclear and tetranuclear cores. *Z. Anorg. Allg. Chem.* **2014**, *640*, 781–789. [[CrossRef](#)]
41. Limanski, E.M.; Drewes, D.; Krebs, B. Sandwich-like polyoxotungstates with indium(III) as a heteroatom synthesis and characterization of the first examples of a new type of anions. *Z. Anorg. Allg. Chem.* **2004**, *630*, 523–528. [[CrossRef](#)]
42. Hussain, F.; Reicke, M.; Janowski, V.; Silva, S.D.; Futuwi, J.; Kortz, U. Some indium(III)-substituted polyoxotungstates of the Keggin and Dawson types. *C. R. Chim.* **2005**, *8*, 1045–1056. [[CrossRef](#)]
43. Zhao, D.; Ye, R.-H. Solvothermal synthesis and structure of a new indium-substituted polyoxotungstate: [(CH<sub>3</sub>)<sub>2</sub>NH<sub>2</sub>]<sub>4</sub>[In<sub>3</sub>(H<sub>2</sub>O)<sub>3</sub>(NO<sub>3</sub>)(A- $\alpha$ -H<sub>3</sub>PW<sub>9</sub>O<sub>34</sub>)<sub>2</sub>].H<sub>2</sub>O. *J. Clust. Sci.* **2011**, *22*, 563–571. [[CrossRef](#)]
44. Brown, I.D.; Altermatt, D. Bond-valence parameters obtained from a systematic analysis of the Inorganic Crystal Structure Database. *Acta Crystallogr.* **1985**, *B41*, 244–247. [[CrossRef](#)]

45. Shannon, R.D.; Prewitt, C.T. Effective ionic radii in oxides and fluorides. *Acta Cryst.* **1969**, *B25*, 925–946. [[CrossRef](#)]
46. Shannon, R.D. Revised effective ionic radii and systematic studies of interatomic distances in halides and chalcogenides. *Acta Cryst.* **1976**, *A32*, 751–761. [[CrossRef](#)]
47. Sheldrick, G.M. A short history of SHELX. *Acta Crystallogr.* **2008**, *64*, 112–122. [[CrossRef](#)] [[PubMed](#)]



© 2016 by the authors; licensee MDPI, Basel, Switzerland. This article is an open access article distributed under the terms and conditions of the Creative Commons Attribution (CC-BY) license (<http://creativecommons.org/licenses/by/4.0/>).